PN35

Temperature gradients within the packed bed affect cumulative supercritical CO_2 extraction plots for oilseeds

José M. del Valle[a,*], Christopher Lorca[a], Luca Fiori[b], & Gonzalo A. Núñez[c]

[a] Dept. Chemical & Bioprocess Eng., Pontificia Universidad Católica de Chile, Santiago
[b] Dept. Civil, Environmental & Mechanical Eng., Università di Trento, Italy
[c] Dept. Chem. & Environmental Eng., San Joaquín Campus, Univ. Técnica Federico Santa María, Santiago, Chile
[*] delvalle@ing.puc.cl

ABSTRACT

Although isothermal conditions are usually assumed during SuperCritical (SC) carbon dioxide (CO_2) extraction of solid substrates, temperature gradients may develop within the packed bed extraction vessel that may affect the extraction rate of the substrate. The cause of these gradients may be differences in temperature between the CO_2 feed and the vessel resulting from residual thermal effects in the vessel wall of unsteady state operations of substrate loading and unloading. The objective of this work was to study the effect of temperature profiles within an extraction vessel on the SC-CO_2 extraction of oil from pelletized cranberry seeds. Temperature gradients were imposed in a vertical, cylindrical extraction vessel (1 dm^3 capacity), by using different temperatures for the CO_2 feed and the vessel wall. In heating experiments, the vessel wall was held at 60 ºC and the CO_2 feed at 40 ºC, whereas in cooling experiments, the two temperatures were reversed. All experiments were performed at 48 MPa, using 4-mm cylindrical oilseed pellets (unitary height-to-diameter ratio) as the substrate. For these experiments, as well as two additional control isothermal (40 or 60 ºC) ones, cumulative oil yield plots were constructed during 4 h extractions using 40 g/min of SC-CO_2. Complimentarily, 3-mm spherical glass beads were used as a model system in heating and cooling experiments. Heat transfer was better when using glass beads than oilseed pellets due to the increased thermal diffusivity and reduced size of the beads as compared to the pellets, and this translated in a faster attainment of steady state conditions during treatment (*ca.* 40-50 min for glass beads as compared to 120-150 min for oilseed pellets). Heat transfer was also better in heating than cooling experiments due to the improved heat transfer coefficient between CO_2 and the particles in the bed. In heating experiments the forced convection was reinforced by the natural convection resulting from the transfer of heat to the up-flowing CO_2. Improved heat transfer translated in smaller axial and radial gradients in temperature in a large section of the extraction vessel located 10 cm above the CO_2 feed in heating than cooling experiments. Overall, temperatures in the packed bed were more affected by the vessel wall than the CO_2 feed. Oil yield following 4 h of extraction increased *ca.* 20% as temperature increased from 40 to 60 ºC as a result of an increase in the operational solubility. The operational solubility equaled the thermodynamic solubility of oil in SC-CO_2 at the wall temperature in isothermal as well as heating and cooling experiments. However, cumulative extraction curves following 1 h of dynamic extraction under heating and cooling conditions began to approach each other, with differences with the corresponding isothermal curves being limited to 5% for the cooling experiment, and to 8% for the heating experiment following 4 h of extraction.

INTRODUCTION

Typically, SuperCritical (SC) carbon dioxide (CO_2) extraction of oilseeds assumes single particle size and shape, constant temperature and pressure, and plug-type flow pattern of CO_2 in the packed bed. These ideal condition assumptions may not apply industrially unlike at laboratory scale. Particularly, temperature gradients may develop within a packed bed due to differences in temperature between the vessel wall and

the CO_2 feed developed during vessel loading [1] and unloading [2]. These temperature variations may be due to Joule-Thompson-type thermal effects associated with CO_2 compression during vessel loading, and CO_2 decompression during vessel unloading, respectively. Small changes in temperature may modify the physical properties of CO_2 (density, viscosity, self-diffusivity) so as to affect the extraction rate. of oilseeds. For example, there may be large variations in oil solubility in CO_2 caused by small a change in temperature; at 48 MPa, it can be estimated to increase from 16.6 ± 3.3 g kg^{-1} oil/CO_2 at 40 ºC to 22.9 ± 4.6 g kg^{-1} at 60 °C [3].

The objective of this work was to study the effect of temperature profiles on local properties of the substrate and SC-CO_2 within an extraction vessel, and the extraction of oil from pelletized seeds.

MATERIALS AND METHODS

Cranberry (*Vaccinium oxycoccus*) seeds were treated in flat D-type pellet mill and manually cut to generate cylindrical pellets of 4 mm diameter and 4 mm height. In addition, spherical glass beads of 3 mm diameter were used as model system. The properties of the materials are summarized in Table 1. True densities (ρ_s) were measured by gas pycnometry. Being pelletized pellets porous particles, there was a difference between ρ_s and ρ_p, the particle density, which was estimated as the ratio between its measured weight and estimated volume (0.050 cm^3). The bulk density (ρ_b) of the two materials, on the other hand, was estimated as the ratio of the weight of the material used to fill the extraction vessel, and the vessel volume (1043 cm^3). The intraparticle porosity (ε_i) of the pellets was estimated using eq. (1), whereas the interparticle bed porosity (ε) of the two materials was estimated using eq. (2) [4]:

$$\varepsilon_i = 1 - \frac{\rho_p}{\rho_s} \quad (1)$$

$$\varepsilon = 1 - \frac{\rho_b}{\rho_p} \quad (2)$$

Values of the specific heat (c_p) and themal conductivity (k) of oilseed pellets reported in Table 1 were estimated using the Choi-Okos correlation for food materials reviewed by Sweat [5], and the resistances-in-parallel correlation proposed by Carson [6] for nonporous unfrozen foods, respectively, which rely on the proximal composition of cranberry seeds. To estimate the proximal composición of cranberry seeds, when used the proximate analysis of a commercial cranberry seed powder [7] in an oil-free basis together with the experimental values of water (6.9%) and oil (20.5%) content.

Table 1. Physical properties of susbtrates used in this work.

Physical property	Oilseed pellets	Glass beads
True density (ρ_s, kg/m^3 × 10^{-3})	1.32	2.49 [8]
Intraparticle porosity (ε_i, −)	0.140	0.000
Bed porosity (ε, −)	0.590	0.420
Specific heat (c_p, kJ kg^{-1} K^{-1})	1.811	0.840 [8]
Thermal conductivity (k, W m^{-1} K^{-1})	0.224	1.20 [8]
Thermal diffusivity* (α, m^2/s × 10^9)	93.8	404

* $\alpha = k\,\rho^{-1}\,c_p^{-1}$

Experiments were carried out in a jacketed, 1 dm^3 (nominal volume) extraction vessel described by Richter *et al.* [8] (Fig. 1). The inlet temperature of the SC-CO_2 fed to the extraction vessel was adjusted using a heat exchanger that used, as service fluid, water that was recycled through a thermostated bath, and was measured using a 1/32”, type-K thermocouple (T1) in the inlet line of the extraction vessel. The temperature of the extraction vessel was adjusted by circulating water through the jacket vessel that was recycled through an independent thermostated bath. To compute the heat transferred to or released from

the vessel wall, we measured the flow of water using a standard rotameter, as well as its temperature using 1/32”, type-K thermocouples in the inlet (T2) and outlet (T3) lines of the vessel jacket. To

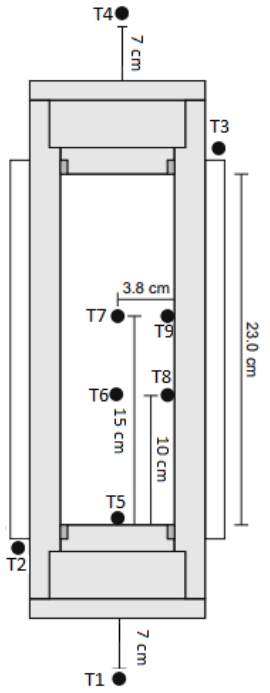

Figure 1. Geometry of 1 dm^3 cylindrical extraction vessel indicating location of thermocouples.

complete the heat balance for the extraction vessel, the exit temperature of the SC-CO_2 was measured using a 1/32”, type-K thermocouple (T4) in its exit line. In the experiments, packed bed temperatures were monitored in five positions along the axis (T5, T6, and T7) and wall (T8 and T9) of the vessel as indicated in Fig. 1, using 1/32’’ type-K thermocouples. All temperature sensors were connected to a data logger.
Heating experiments were performed after thermal equilibration of the packed bed extractor to 60 ºC by feeding 40 g/h of SC-CO_2 at 40 ºC and 48 MPa (U = 0.16 mm/s) while circulating water at 60 ºC through the vessel jacket. Cooling experiments, on the other hand, were carried out equilibrating the packed bed extractor and keeping its wall at 40 ºC, and feeding 40 g/h of SC-CO_2 at 60 ºC and 48 MPa (U = 0.14 mm/s). Table 2 summarizes the physical properties of SC-CO2 at test conditions that where estimated using the REFPROP program [9] for pure CO_2 at test conditions under the assumption that the dissolved oil (low solubility) does not affect them [10]. The only exception was the binary diffusion coefficient of the oil in SC-CO_2, or the oil diffusivity (D_{12}), which was estimated using the correlation of Funazukuri *et al.* [11] using triolein as a representative component in the vegetable oil [3].

Table 2. Physical properties of supercritical CO_2 at test conditions used in this work.

Physical property	40 ºC and 48 MPa	60 ºC and 48 MPa
Density (ρ, $kg/m^3 \times 10^{-3}$)	0.985	0.927
Coefficient of thermal expansion (β, $K^{-1} \times 10^5$)	3.194	3.003
Viscosity (μ, mPa s)	0.115	0.097
Specific heat (c_p, kJ kg^{-1} K^{-1})	1.765	1.768
Thermal conductivity (k, W m^{-1} K^{-1})	0.126	0.113
Dimensionless Prandtl number* (Pr, −)	1.613	1.514
Thermal diffusivity (α, $m^2/s \times 10^8$)	7.281	6.913
Oil diffusivity (D_{12}, $m^2/s \times 10^9$)	2.514	3.086

* $Pr = c_p\, \mu^{-1}\, k^{-1}$

Heating and cooling experiments were carried out with oilseed pellets or glass beads. In addition, control isothermal experiments were carried out with oilseed pellets at 40 or 60 ºC and 48 MPa. In experiments with oilseed pellets, data was collected to construct cumulative extraction plots of oil yield *versus* specific CO_2 consumption. All experiments were extended up to 4 h, and performed in duplicate.

RESULTS

Fig. 2 summarizes results for temperature profiles in heating and cooling experiments for glass beads and oilseed pellets. In heating experiments using glass beads (Fig. 2.A), temperatures within the packed bed ranged from *ca.* 46 ºC near the CO_2 inlet to *ca.* 57−59 ºC in all other positions with a maximum near the hot vessel wall and a minimum near the axis, both far from the entrance. The CO_2 temperature at the entrance of the packed bed is slightly higher than the feed temperature (6 ºC above it) due to its heating in the thick and hot (60 ºC) bottom cap of the extraction vessel. In a short distance (*ca.* 10 cm) from the entrance, the SC-CO_2 stream equilibrates to the initial temperature of the packed bed contents due to heat transfer from the hot glass beads and the vessel wall. Glass beads would cool down as affected by the passing CO_2 stream, but this effect would be partially offset by the heat transferred through the vessel wall by the heating media in the vessel jacket (water at 60 ºC). A steady state condition is reached after *ca.* 40 min that is characterized by limited temperature fluctuations of about ±1 ºC.

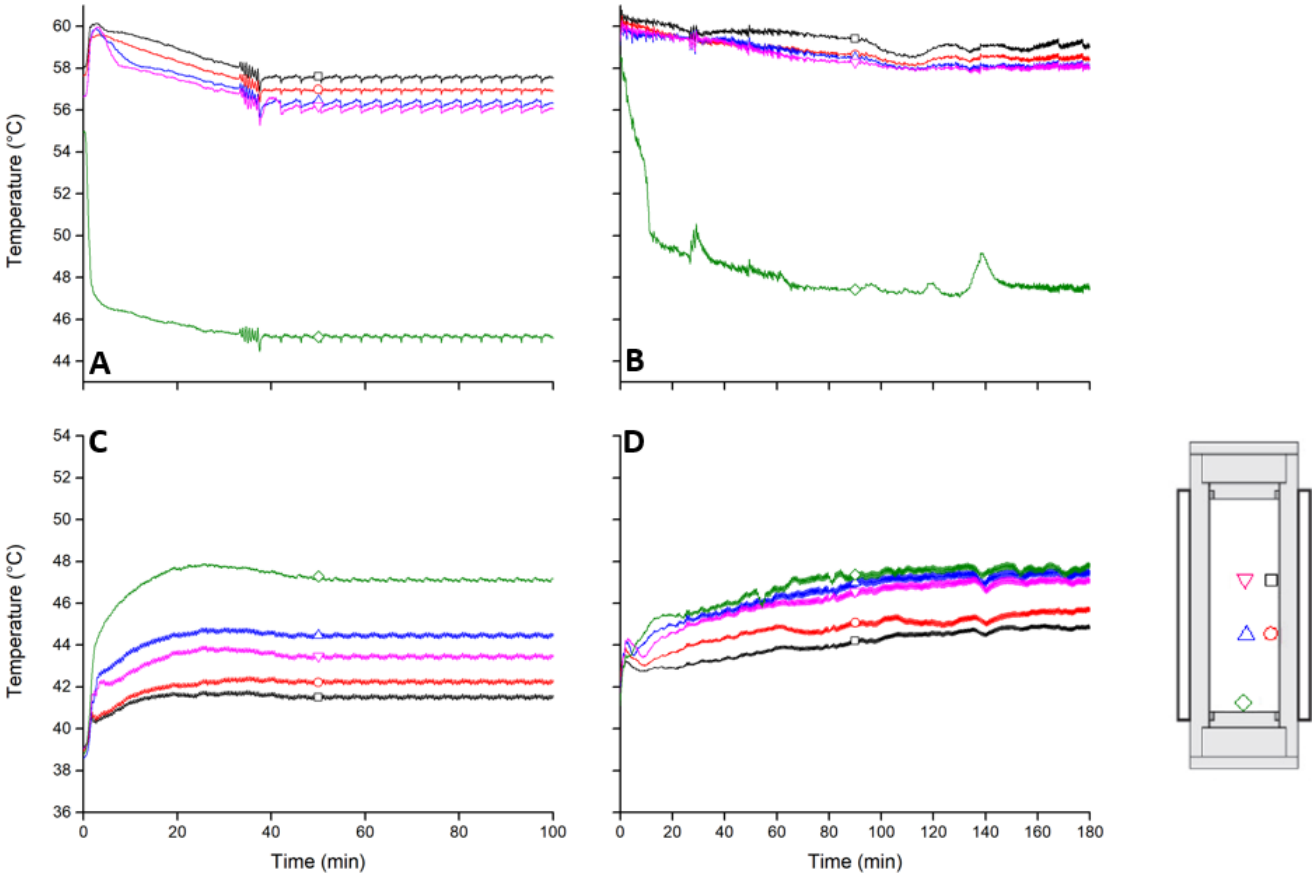

Figure 2. Temperature evolution in five positions within 1-dm^3 extraction vessel packed with (**A**,**C**) 3-mm glass beads or (**B**,**D**) 4-mm cylindrical oilseed pellets during (**A**,**B**) heating-type experiments (CO_2 feed at 40 ºC, vessel wall at 60 ºC) or (**C**,**D**) cooling-type experiments (CO_2 feed at 60 ºC, vessel wall at 40 ºC).

Trends in heating experiments for oilseed pellets (Fig. 2.B) are similar to those observed for glass beads (Fig. 2.A) with small differences. Differences relate to the noisier nature of the temperature fluctuations both in short-time and large-time scales (*cf.* perturbations at 20 and 130 min in Fig. 2.B, particularly at

the entrance of the extraction vessel), and the longer period to attain steady state conditions (*ca.* 120 min in the new case) when using oilseed pellets than glass beads. This may be due to the improved packing homogeneity and thermal properties of the glass beads as compared to the oilseed pellets.

In cooling experiments using glass beads (Fig. 2.C), on the other hand, temperatures within the packed bed ranged from *ca.* 48 ºC near the CO_2 inlet to *ca.* 41−44 ºC in all other positions (a minimum at the vessel wall and a maximum at the axis, both far from the CO_2 entrance). As before, steady state conditions are reached in about 50 min, but there are striking differences as compared to the heating experiments (Fig. 2.A) in that temperatures are more equally spaced in the bottom 15 cm of the extraction vessel, which is the distance along the vessel wall that the CO_2 stream takes to cool down to the wall temperature. Due to constraints to heat transfer within the packed bed, a gradient of *ca.* 2−3 ºC persist between the axis and the wall of the vessel in cooling experiments (Fig. 2.C) as compared to 0.5−1 ºC in heating experiments (Fig. 2.A).

Results for cooling experiments using oilseed pellets (Fig. 2.D) are a consequence of trends previously noted for differences in substrate properties in the case of heating experiments (Fig. 2.B using oilseed pellets *versus* Fig. 2A using glass beads), as well as for differences between type of experiment using glass beads (Fig. 2.C for cooling *versus* Fig. 2.A for heating). Indeed, attainment of steady state conditions in slower for cooling of SC-CO_2 in packed beds with oilseed pellets (*ca.* 150 min) than glass beads (*ca.* 50 min). Also, the temperature of the SC-CO_2 at the entrance of the packed bed is not as separated from temperatures at ≥10 cm from the entrance in cooling experiments (≤4 ºC) than heating experiments (≥10 ºC). Finally, temperatures in the middle section of the extraction vessel in the axial direction and across the vessel in the radial direction varied less in heating (≤1 ºC) than cooling (≥3 ºC) experiments.

Extraction rate and yield after a 4-h dynamic extraction increase as temperature increases from 40 to 60 ºC (Fig. 3), possibly due to the increase in the solubility of the oil in SC-CO_2 at a pressure above the solubility crossover (*ca.* 31 MPa [3]), below which the trend reverses and solubility decreases as temperature increases. Cumulative extraction curves in heating and cooling experiments were intermediate between the two isothermal experiments. The initial slope of the cumulative extraction plots in Fig. 3 were 18.5 g kg^{-1} oil/CO_2 for packed beds equilibrated to 40 ºC in the static extraction period, and 24.8 g kg^{-1} oil/CO_2 for packed beds equilibrated to 60 °C, which are close but slightly above the corresponding solubility values at 48 MPa informed in the introduction. The effect of the entrance of SC-CO_2 to the extraction vessel at a different temperature from that used for equilibration and static extraction was noted after *ca.* 1 h of dynamic extraction, and this resulted in a slight increase (cooling experiment) or decrease (heating experiment) of about 5 to 8% in oil yield following 4 h of extraction. From Fig. 3, it is apparent that the extraction rate was completely determined by the wall temperature initially, and that the cumulative extraction curve deviated slightly thereafter as affected by the CO_2 feed temperature. Following 4 h of dynamic extraction, the pelletized substrate is not fully exhausted, and differences in extraction rate related mainly to differences in oil solubility translate in a difference in yield of 19.3% between isothermal experiments at 40 or 60 ºC and 48 MPa.

DISCUSSION

The SC-CO_2 extraction of pelletized oilseeds at 48 MPa following a static extraction period is almost fully determined by oil solubility in CO_2 at the equilibration temperature (Fig. 3). Indeed, the slope of the cumulative extraction curves following equilibration at 40 or 60 ºC is about 2 g kg^{-1} oil/CO_2 above the corresponding thermodynamic solubility values estimated using the equation of del Valle *et al.* [3] but within the ±30% error predicted by the authors. This was expected, because solubility determines equilibration during the long static extraction period required to homogenize temperature within the relatively large extraction vessel used in our experiments, and because using a very small superficial velocity during the dynamic extraction period gave time (*ca.* 24 to 27 min) for the passing SC-CO_2 stream to equilibrate with the pelletized substrate. Transient effects associated with the entrance of SC-CO_2 at a different temperature from that of the extraction vessel walls start manifesting only after about

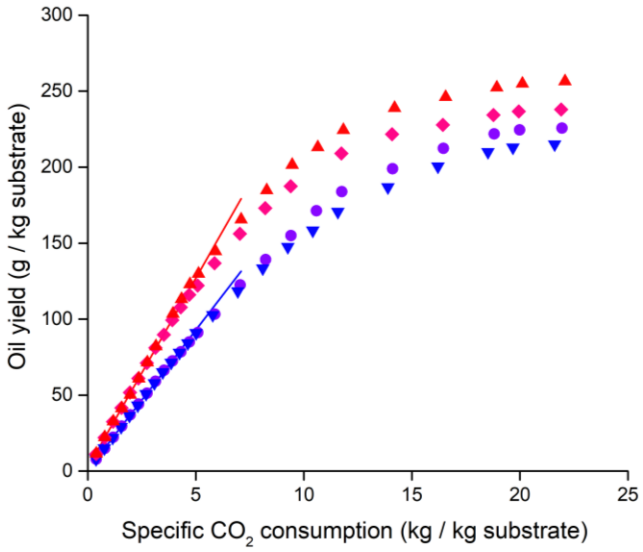

Figure 3. Cumulative oil extraction curves for 4-mm cylindrical oilseed pellets using SC-CO_2 at 48 MPa as a function of temperature: (red up-triangles) 60 ºC (isothermal); (pink diamonds) heating-type experiment (CO_2 feed at 40 ºC, vessel wall at 60 ºC); (violet circles) cooling-type experiment (CO_2 feed at 60 ºC, vessel wall at 40 ºC); and, (blue down-triangles) 40 ºC (isothermal). Lines represent operational solubities depending on vessel wall temperature: (red) 60 ºC; and (blue) 40 ºC.

1 h extraction when steady-state axial- and radial-gradients in temperature can be expected to be established within the packed bed (Fig. 2B and Fig. 2D). Gradients are more limited under heating (Fig. 2A and Fig. 2B) than cooling (Fig. 2A and Fig. 2B) conditions and this explains the larger differences between the two upper curves in Fig. 3 (differences in yield of 8% following 4 h of extraction) than between the two lower curves (differences in yield of 5% after the same time).

Results of extraction rate can be explained by system temperature that was more affected by the vessel wall than the CO_2 feed because the steel and glass beads or oilseeds pellets act as reservoir of heat that is conducted faster through the high-thermal conductivity stainless steel of the vessel than the solid substrate and the inter- and intraparticle fluid.

Heat transfer within a packed bed extraction vessel is a very complex phenomenon that considers several interconnected convection and conduction mechanisms involving the vessel wall and its contact with the substrate particles and the passing SC-CO_2 stream, as well as the contact between the particles, and between the particles and the passing SC-CO_2 stream [12]. These heat transfer mechanisms are, in turn, affected by the temperature gradients, the arrangement and physical properties of the packed bed particles, and the movement and physical properties of the SC-CO_2 stream [12]. We believe that the differences between heating and cooling experiments, as well as the differences between glass beads and oilseed pellets that are reported in Fig. 2 are due mainly to differences in the heat transfer coefficient (h) between the passing SC-CO_2 stream and the particles, and differences in thermal diffusivity (α), size, and shape between the glass beads and oilseed pellets (Table 1). Heat transfer rate increases as a result of an increase in the value of h, that is higher in heating than cooling experiments due to the positive influence of natural convection phenomena. On the other hand, thermal gradients within substrate particles dissipate faster as values of α increase and/or as the size of the particles decreases, being these two factors better for glass beads than oilseed pellets. Faster heat transfer within the packed bed and faster dissipation of thermal gradients within substrate particles result in smaller differences in temperature in the middle section of the extraction vessel in the axial direction (10 to 15 cm from the bottom), and across the vessel (in the radial direction), as well as faster attainment of steady state conditions. Considering these indications, the fastest heat transfer is evidenced in the heating experiment using a packed bed of glass beads (Fig. 2.A).

In transient heat transfer within solid particles, temperature gradients are defined by a dimensionless time or Fourier time (*Fo*), which is defined by Eq. (3):

$$Fo = \frac{\alpha\, t}{d_p^2}. \quad (3)$$

For any given time, the dimensionless time increases as α increases or the characteristic dimension of the particle (d_p) decreases. Considering the differences between substrate particles informed in Table 1, the actual time required to reach an equivalent temperature profile should be roughly 10 to 15 longer for 4-mm cylindrical oilseed pellets with a unitary shape factor (same height as diameter), whose surface is equivalent to that of a sphere of 4.9 mm diameter, than 3-mm spherical glass beads. These calculations do not take into account the effect of temperature on the thermal diffusivity of the two materials. Furthermore, in the case of the oilseed pellets the calculation does not take into account the effect of the intraparticle porosity (void volume) that is filled with SC-CO_2 at process conditions, nor transient changes associated with oil extraction that increases the void volume with time, and changes the chemical make-up of the substrate particle that is used to estimate its heat capacity and thermal conductivity.

When feeding SC-CO_2 from the bottom of a vertical extraction vessel, as in our experiments, natural convection contributes to convective heat transfer when the vessel wall and the packed substrates are at a temperature above the one of SC-CO_2 as in the heating experiments (a decrease in CO_2 density with temperature causes solvent upflow in the presence of a gravitational field). However, natural convection detracts from convective heat transfer in the cooling experiments when the wall and substrate are colder than the SC-CO_2, because the increase in CO_2 density with the decrease in temperature causes solvent downflow in the gravitational field. The relative magnitude of the forced and natural convection phenomena depends on the relative magnitude of the dimensionless Reynolds [*Re*, Eq. (4)] and Grashof [*Gr*, Eq. (5)] numbers, respectively, as indicated by the magnitude of the Re/Gr^2 ratio.

$$Re = \frac{U\, \rho\, d_p}{\mu} \quad (4)$$

$$Gr = \frac{g\, \beta\, \rho^2 \left(T_w - \bar{T}\right)}{\mu^2} \quad (5)$$

Based on values informed in Table 3, being in our particular case $1 << 1.51\times10^8 \leq Gr/Re^2 \leq 3.07\times10^8$, natural convection cannot be neglected as compared to forced convection [13]. Under these conditions, values of *h* can be estimated using the correlation proposed by Guardo *et al.* [14] for cases where both forced convection (FC) and natural convection (NC) contribute to heat transfer in packed beds operating with SC-CO_2, Eq. (6), where the plus sign is used when FC is assisted by NC (in heating experiments), whereas the minus sign is used when FC is opposed by NC (in cooling experiments):

$$Nu = Nu_0 + \left| Nu_{CF} \pm \left(Nu_{CN} - Nu_0 \right) \right|, \quad (6)$$

where $Nu_0 = 2$,

$Nu_{CF} = 0.269 \times Re^{0.88} \times Pr^{0.30}$, and

$Nu_{CN} = Nu_0 + 0.001 \times Gr^{0.330} \times Pr^{0.574}$.

Final estimates for the values of *h* in the experiments presented in Fig. 2 using Eq. (6) are summarized in Table 3, that suggest increases in *h* when changing from cooling to heating experiments, and when replacing glass beads by oilseed pellets as the substrate, as expected. The same as in the case of thermal diffusivity analysis, we did not account for the changes in *h* brought about by the changes in the porosity and composition of the substrate, nor we did account for changes in h along the extraction vessel brought about by changes in temperature resulting the heating or cooling of SC-CO_2, that would decrease the effect of natural convection on the heat transfer.

Table 3. Estimation of the heat transfer coefficient between the particles and CO_2 at the entrance of the packed bed extractor.

Parameter	Glass beads	Oilseed pellets

	Cooling	Heating	Cooling	Heating
Re (−)	5.06	4.27	6.35	6.05
$Gr \times 10^{-9}$ (−)	6.52	5.52	6.52	5.52
$Gr / Re^2 \times 10^{-8}$ (−)	2.54	3.07	1.61	1.51
Nu_{CF} (−)	3.17	3.48	3.46	3.80
Nu_{CN} (−)	2.77	2.37	2.77	2.37
h (W m^{-2} K^{-1})	220	211	173	171

ACKNOWLEDGEMENTS
This work was funded by Chilean scientific agency FONDECYT (Project #1150623).

REFERENCES
[1] ZABOT G.L., MORAES M.N., PETENATE A.J., MEIRELES M.A.A., Influence of the bed geometry on the kinetics of the extraction of clove bud oil with supercritical CO_2, The Journal of Supercritical Fluids, Vol. 93, 2014, p. 56−66.
[2] RICHTER E.A., DEL VALLE J.M., NÚÑEZ G.A., Thermodynamic properties of CO_2 during controlled decompression of supercritical extraction vessels, The Journal of Supercritical Fluids, Vol. 98, 2015, p. 102−110.
[3] DEL VALLE J.M., DE LA FUENTE J.C., UQUICHE E.L., A refined equation for predicting the solubility of vegetable oils in high-pressure CO_2, The Journal of Supercritical Fluids, Vol. 67, 2012, pp. 60−70.
[4] MAUGUET M.C., MONTILLET A., COMITI J., Macrostructural characterization of granular activated carbon beds, Journal of Materials Science, Vol. 40, 2005, p. 747−755.
[5] SWEAT V.E., Thermal properties of foods, in: RAO M.A., RIZVI S.S.H. (Eds.), Engineering Properties of Food (2nd ed.), Marcel Dekker, Inc., New York, 1994, p. 99–138.
[6] CARSON J.K., Review of effective thermal conductivity models for foods, International Journal of Refrigeration, Vol. 29, 2006, p. 958–967.
[7] https://phytotherapy.com.au/wp-content/uploads/2016/09/Organic-Cranberry-Seed-Powder-2-PACs.pdf
[8] RICHTER E.A., MURIAS M.S., DEL VALLE J.M., Heat transfer and venting rate during controlled decompression of supercritical extraction vessels, The Journal of Supercritical Fluids, Vol. 120, 2017, p. 275−284.
[9] LEMMON E.W., HUBER M.L., McLINDEN M.O., NIST Standard Reference Database 23: Mini-reference Fluid Thermodynamic and Transport Properties (REFPROP), Version 9.0, 2007.
[10] DEL VALLE J. M., Extraction of natural compounds using supercritical CO_2: Going from the laboratory to the industrial application, The Journal of Supercritical Fluids, Vol. 96, 2015, p. 180–199.
[11] FUNAZUKURI T., TORIUMI M., YUI K., KONG C.Y., KAGEI S., Correlation for binary diffusion coefficients of lipids in supercritical carbon dioxide, in: 9th International Symposium on Supercritical Fluids (ISSF 2009), Arcachon, France, May 18-20, 2009.
[12] WAKAO N., KAGUEI S., Heat and Mass Transfer in Packed Beds, Gordon and Breach Science Publishers, New York, NY, 1982.
[13] INCROPERA F.P., DeWITT D.P., Fundamentals of Heat and Mass Transfer (5th. Ed.), John Wiley & Sons, Hoboken, NJ, 2002.
[14] GUARDO A., COUSSIRAT M., RECASENS F., LARRAYOZ M.A., ESCALER X., CFD study on particle-to-fluid heat transfer in fixed bed reactors: Convective heat transfer at low and high pressure, Chemical Engineering Science, Vol. 61, 2006, p. 4341-4353.